J Physiol 586.24 (2008) pp 6007–6019

The Journal of Physiology

Regulation of mouse lung development by the extracellular calcium-sensing receptor, CaR

Brenda A. Finney[1], Pierre M. del Moral[2], William J. Wilkinson[1], Sebastien Cayzac[1], Martin Cole[1], David Warburton[2], Paul J. Kemp[1] and Daniela Riccardi[1,3]

[1]*School of Biosciences, Museum Avenue, Cardiff University, Cardiff, CF10 3AX, UK*
[2]*Saban Research Institute of Children's Hospital, Los Angeles, CA 90027, USA*
[3]*Cardiff Institute of Tissue Engineering and Repair (CITER), Museum Avenue, Cardiff University, Cardiff, CF10 3AX, UK*

Postnatal lung function is critically dependent upon optimal embryonic lung development. As the free ionized plasma calcium concentration ($[Ca^{2+}]_o$) of the fetus is higher than that of the adult, the process of lung development occurs in a hypercalcaemic environment. In the adult, $[Ca^{2+}]_o$ is monitored by the G-protein coupled, extracellular calcium-sensing receptor (CaR), but neither its ontogeny nor its potential role in lung development are known. Here, we demonstrate that CaR is expressed in the mouse lung epithelium, and that its expression is developmentally regulated, with a peak of expression at embryonic day 12.5 (E12.5) and a subsequent decrease by E18, after which the receptor is absent. Experiments carried out using the lung explant culture model *in vitro* show that lung branching morphogenesis is sensitive to $[Ca^{2+}]_o$, being maximal at physiological adult $[Ca^{2+}]_o$ (i.e. 1.0–1.3 mM) and lowest at the higher, fetal (i.e. 1.7 mM) $[Ca^{2+}]_o$. Administration of the specific CaR positive allosteric modulator, the calcimimetic R-568, mimics the suppressive effects of high $[Ca^{2+}]_o$ on branching morphogenesis while both phospholipase C and PI3 kinase inhibition reverse these effects. CaR activation suppresses cell proliferation while it enhances intracellular calcium signalling, lung distension and fluid secretion. Conditions which are restrictive either to branching or to secretion can be rescued by manipulating $[Ca^{2+}]_o$ in the culture medium. In conclusion, fetal Ca_o^{2+}, acting through a developmentally regulated CaR, is an important extrinsic factor that modulates the intrinsic lung developmental programme. Our observations support a novel role for the CaR in preventing hyperplastic lung disease *in utero*.

(Received 17 August 2008; accepted after revision 24 October 2008; first published online 27 October 2008)
Corresponding author D. Riccardi and P. J. Kemp: Biomedical Sciences Building, Museum Avenue, Cardiff CF10 3AX, UK. Email: riccardi@cf.ac.uk and kemp@cf.ac.uk

Postnatal lung function is crucially dependent upon a finely controlled embryonic developmental programme. Lung development *in utero* is a stereotypic process of budding and branching that ends with a mature lung capable of gas exchange within minutes of birth. In the mouse, branching morphogenesis takes place during the pseudoglandular phase, between embryonic day (E) 11.5 and E16.5, when the lung's peripheral bud network rapidly branches to form the acinar tubules (Whitsett *et al.* 2004; Warburton, 2008). While lung organogenesis is under the control of many genetic and epigenetic factors, lung growth is largely dependent on environmental stimuli. Integration of both sets of signals ultimately determines postnatal lung physiology or pathology (Warburton & Olver, 1997).

The process of lung development occurs in a hypercalcaemic environment, where the free ionized plasma calcium concentration ($[Ca^{2+}]_o$) of the fetus is ~1.7 mM (Kovacs & Kronenberg, 1997), and is therefore above the adult level of between 1.0 and 1.3 mM (Brown, 1991). Experiments carried out in murine models (Kovacs *et al.* 1998) have demonstrated that this relative hypercalcaemia is independent of the maternal $[Ca^{2+}]_o$ and is influenced by the extracellular calcium-sensing receptor (CaR).

The CaR is a member of the G-protein coupled receptor (GPCR) superfamily, and is the master regulator of the adult serum Ca^{2+} homeostatic system (Brown & Macleod, 2001). Activation of the CaR is linked to a phospholipase C-mediated increase in intracellular calcium concentration ($[Ca^{2+}]_i$) in almost every system expressing the CaR (Brown & Macleod, 2001). Compatible with its role in the control of systemic $[Ca^{2+}]_o$ is the fact that CaR is highly expressed in organs involved in extracellular free ionized calcium (Ca_o^{2+}) homeostasis

DOI: 10.1113/jphysiol.2008.161687

(Brown *et al.* 1993; Riccardi *et al.* 1995; Brown & Macleod, 2001; Dvorak *et al.* 2004). In addition, CaR is also expressed in a number of tissue types and cell systems which have no apparent link with mineral ion metabolism (Bruce *et al.* 1999), including the developing central and peripheral nervous system (Vizard *et al.* 2008). Previous work has been unable to detect CaR expression in adult lung (Brown *et al.* 1993; Riccardi *et al.* 1995), but no study has specifically investigated prenatal expression of this receptor. However, patients carrying heterozygous inactivating mutations in the CaR gene show interstitial lung disease and reduced diffusing capacity with age, which are independent of smoking habits (Auwerx *et al.* 1985, 1987), but whether the CaR has a functional role in lung development has not been addressed. Thus, using the organ explant culture model, it was the scope of the current work to study the effects of $[Ca^{2+}]_o$ on lung branching morphogenesis, and to test the involvement of the CaR in this process.

Methods

Ethical approval

Mice (C57/Bl6) were housed conventionally with 12 h light:dark cycle and were allowed access to food and water *ad libitum*. For the qPCR experiments, mice were killed by CO_2 inhalation in accordance with the Institutional Animal care and Use Committee Regulations (Children's Hospital Los Angeles); 24 neonates from eight time-mated female mice and three postnatal mice were used for these studies. All other animal procedures were carried out in the UK, were approved by local ethical review and conformed to UK Home Office Regulations. For these experiments, 64 time-mated pregnant adult females were killed by CO_2 inhalation, after which their uteri were removed. The embryos ($n = 329$) were then dissected from their membranes and decapitated.

Reagents

Unless otherwise stated, all reagents were from Sigma-Aldrich, Poole, UK.

RNA isolation and quantitative polymerase chain reaction (PCR)

RNA was purified from pooled lung samples aged between E11.5–E18.5 and postnatal (P) day 10 using RNeasy kits (Qiagen, Crawley, UK). One microgram of RNA was reverse-transcribed using the iScript select kit (Bio-Rad, Hemel Hempstead, UK). Quantitative PCR (qPCR) reactions to amplify 18S and CaR RNAs were carried out separately using a Light cycler (Roche Diagnostics Corp., Indianapolis, IN, USA). Primers specific for CaR (NM_013803.2) and 18S (NR_003278.1) sequences were designed to be used in conjunction with Roche Universal Probe Library, using the Roche Assay Design Center (www.roche-applied-science.com). The Universal Probes and primer sequences employed in the qPCR reactions were as follows. 18S Universal probe #55 with the primers: 18S forward, 5′-AAAT-CAGTTATGGTTCCTTTGGTC-3′; 18S reverse, 5′-GCTC-TAGAATTACCACAGTTATCCAA-3′. CaR Universal probe no. 32, with the intron-spanning primers: CaR forward, 5′-GGTCCTGTGCAGACATCAAG-3′; CaR reverse, 5′-CCGCACTCATCGAAGGTC-3′.

All qPCR reactions were carried out using the same cycling parameters, which were 5 min activation at 95°C, followed by 40 cycles of 95°C/20 s, 60°C/20 s, 72°C/10 s.

Lung explant culture and time-lapse microscopy

Lungs were explanted from E12.5 mice and cultured in chemically defined, serum-free conditions according to previously published protocols (De Langhe *et al.* 2005; Del Moral *et al.* 2006). Branching morphogenesis was quantified, and is shown in the text and figure legends, as 'increase in branching (%)'. The number of terminal buds at 0, 24 and 48 h was counted and branching increase (%) at each time point was calculated as: $(Branches_{24h\ or\ 48h} - Branches_{0h})/Branches_{0h} \times 100$. Images were captured with a dissecting microscope equipped with a digital camera (Leica Microsystems Ltd, Milton Keynes, UK). For time-lapse microscopy, E12.5 lungs were placed on Transwell filters (Corning, Reading, UK) and cultured in an Incucyte cell-imager (Essen Instruments, London). Images were acquired every 30 min for 48 h. $[Ca^{2+}]$ in Dulbecco's modified Eagle's medium (DMEM)–F12 was adjusted from 1.05 mM to the concentrations stated in text and figures using appropriate amounts of EGTA or $CaCl_2$, and the final concentration was measured with a blood gas analyser (ABL800 FLEX, Radiometer Ltd, Crawley, UK). The positive allosteric modulator of the CaR R-568 (Amgen, Thousand Oaks, CA, USA), the PI3 kinase (PI3K) inhibitor LY294002, the mitogen-activated protein kinase (MAPK) inhibitor BIRB 796, the extracellular-regulated protein kinase 1/2 (ERK1/2) inhibitor U0126, and the mitogen-activated protein kinase kinase (MEK) inhibitor PD98059 were added to the culture medium for 48 h in culture while the phospholipase C (PLC) inhibitor U73122 was added to the culture medium at time 0 h and removed after 24 h. The drugs were added to the culture medium to give the final concentrations defined in the text and figures. DMSO vehicle controls at 0.1% or 0.05% were always performed in parallel, as indicated.

Immunohistochemistry

Paraformaldehyde-fixed, paraffin-embedded tissues were antigen-retrieved with citrate buffer (Riccardi *et al.* 1998). Briefly, the optimized protocol was as follows. Slides were incubated in 3% bovine serum albumin (BSA) in phosphate-buffered saline (PBS) containing 0.1% Triton X-100 for 1 h at room temperature. Primary antibodies (1/400) were diluted in PBS containing 1% BSA, 3% Seablock (Stratech Scientific, Soham, UK), 0.1% Triton X-100 and applied to the slides for 12–16 h at 4°C. Three affinity-purified, rabbit polyclonal antibodies, which recognize separate epitopes in the amino terminus of the CaR, were used. Our 733 antiserum has been characterized previously (Riccardi *et al.* 1998) whilst the IMG-71169 and PA1–934A antisera are commercially available from Imgenex (Cambridge Bioscience, Cambridge, UK) and Affinity BioReagents (Golden, CO, USA), respectively. Detection of primary antibody binding using reagents from Envision Diaminobenzidine kit (DAKO, Ely, UK). The secondary, horseradish peroxidase-conjugated antibody was applied for 30 min at room temperature, immunoreactivity was visualized with diaminobenzidine, and the tissue was counterstained with haematoxylin. The specificity of the immunostaining was confirmed by performing preabsorption of the antiserum with its relative antigen (antiserum 733), by using the pre-immune serum (antiserum IMG-71169), by the substitution of primary antibody with an irrelevant IgG rabbit (IgG substitution) and by omission of the primary antibody (all antisera).

Proliferating cells were detected using a rabbit polyclonal antibody against phospho-histone H3 (Cell Signalling Technology Inc., Danvers, MA, USA) whilst apoptotic cells were detected using the Apoptag peroxidase *in situ* apoptosis detection kit (Flowgen Bioscience Ltd, Wilford, UK). Five 100× photomicrographs were taken from two sections per lung (5 sections apart, to minimize the risk of double counting cells). The number of positive cells was expressed as a percentage of total cell number within each photomicrograph.

Calcium imaging

From E12.5 lungs, mesenchyme was gently removed from the epithelium using forceps and the epithelial buds were cultured for 24 h as above but with the addition of 1% fetal calf serum (Invitrogen, Paisley, UK). Epithelia were loaded with 6 μM fura-2 acetoxymethyl ester (Molecular Probes, Eugene, OR, USA) for 60 min at 37°C, as previously described (Ward *et al.* 2002). The epithelial buds were then placed on glass coverslips and covered with Nucleopore filters (Whatman International Ltd, Maidstone, Kent, UK) to prevent movement. These were placed in a perfusion chamber mounted upon a Nikon Diaphot equipped with a Cairn monochromotor-based fluorescence system (Cairn Instruments, Faversham, UK) and were continuously superfused with a solution containing (in mM): 135 NaCl, 5 KCl, 0.8 $CaCl_2$, 0.8 $MgCl_2$, 5 Hepes, 10 glucose, pH 7.4. R-568 and carbachol were added to this solution to the final concentrations of 100 nM and 10 μM, respectively. Fura-2 was alternately excited at 340 and 380 nm. Images at 510 nm were acquired at 0.2 Hz by a slow-scan CCD camera (Kinetic Imaging Ltd, Nottingham, UK). Following background subtraction, emission ratios (340/380) were calculated off-line using the Andor IQ 1.3 software package (Andor Technology, Belfast, UK).

Electrophysiology

Transepithelial potential difference (PD) was recorded at 20–22°C using an Axon MultiClamp 700A (Molecular Devices, Sunnyvale, CA, USA) in current clamp mode. Lung explants, attached to filters, were placed in a recording chamber mounted on an Olympus CK41 inverted microscope (Olympus, Southall, UK) and secured with nylon mesh held taut by a platinum ring. The recording chamber was then filled with a solution containing (in mM): 135 NaCl, 5 KCl, 1.2 $MgCl_2$, 1 $CaCl_2$, 5 Hepes, 10 glucose, pH 7.4. 5 MΩ borosilicate glass electrodes (World Precision Instruments, Stevenage, UK), filled with 0.4% trypan blue solution (Invitrogen) in 0.85% saline, were carefully pushed into a lumen terminal whilst maintaining positive pressure on the electrode. When trypan blue was visualized in the lumen, it was considered that lumen access had been achieved and the positive pressure was immediately removed. PD was recorded after a 5 min equilibration period. The ground electrode was of Ag–AgCl and was placed ∼5 mm from the explant.

Statistics

Data are presented as the mean (from multiple pooled experiments where indicated) with the standard error of the mean (S.E.M.). Significance was determined using one-way ANOVA with Tukey's *post hoc* test.

Results

CaR expression is developmentally regulated in the mouse lung

CaR protein expression was detected in the lung as early as E10.5 (Fig. 1*A*). The ontogeny was similar when any of the three antibodies defined in Methods were employed. For brevity, and since the three antibodies generated the same ontogenic pattern, only the data using 733 are presented in Fig. 1. From E10.5 to E12.5, CaR protein became apparent

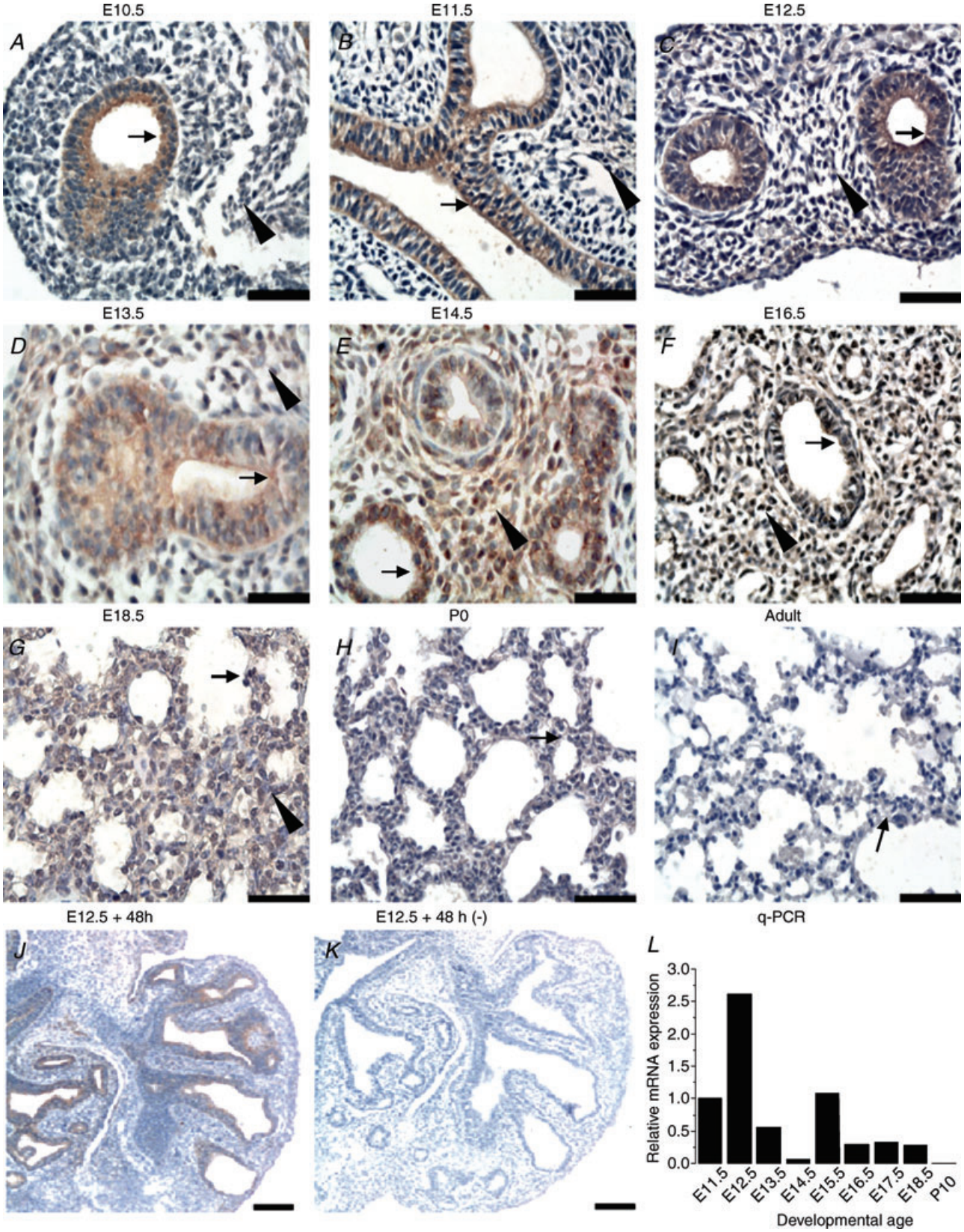

exclusively in the epithelium (Fig. 1*A*–*C*). From E13.5 to E18.5, expression in the epithelium was maintained, albeit in gradually decreasing amounts, through to E18.5 (Fig. 1*D*–*G*). As development proceeded, CaR expression also became apparent in the mesenchyme, between E13.5 and E18.5 (Fig. 1*D*–*G*). In P0 and adult tissue, CaR expression was absent (Fig. 1*H* and *I*). Pre-absorption of the primary antibody with the antigenic peptide (733), substitution of a primary antibody (IMG-71169) with preimmune serum (Fig. 1*K*), or replacement of any of the primary antibodies with an irrelevant IgG (data not shown) was used to demonstrate the specificity of the signals and resulted in the absence of CaR immunoreactivity. In agreement with the protein data, steady-state mRNA level was maximal at E12.5 (Fig. 1*L*).

Branching morphogenesis is sensitive to $[Ca^{2+}]_o$ through activation of the CaR

CaR expression in E12.5 lung explants was maintained for the duration of culture (48 h) and was detected in the epithelium (Fig. 1*J*). E12.5 lung explants were incubated in the presence of different $[Ca^{2+}]_o$, spanning the CaR sensitivity range (Brown & Macleod, 2001). Physiologically, ∼1.2 and ∼1.7 mM correspond to the adult and fetal serum $[Ca^{2+}]_o$, respectively (Kovacs & Kronenberg, 1997). Figure 2*A* shows that lung branching morphogenesis was exquisitely sensitive to $[Ca^{2+}]_o$ during the 48 h in culture, with concentrations of 1.05–1.2 mM having a permissive role on lung branching when compared to the higher, 1.7 mM $[Ca^{2+}]_o$. Figure 2*B* shows that at 48 h branching morphogenesis was maximal at the physiological adult $[Ca^{2+}]_o$ of 1.05–1.2 mM, with the number of terminal lung branches in 1.05 mM and 1.2 mM Ca_o^{2+} being increased by 123.3 ± 4.5% ($n = 54$) and by 109.7 ± 3.1% ($n = 88$), respectively. In contrast, branching was reduced to 62.2 ± 4.4% ($n = 45$) when $[Ca^{2+}]_o$ was 1.7 mM. A comparable reduction in lung branching was also seen in the presence of 2 mM Ca_o^{2+} (37.1 ± 8.8%, $n = 11$) and 2.5 mM Ca_o^{2+} (54.7 ± 4.2%, $n = 45$), suggesting that the influence of $[Ca^{2+}]_o$ on embryonic lung branching is effectively saturating between 1.7 and 2.0 mM (Fig. 2*B*). To demonstrate an involvement of the CaR in mediating these inhibitory effects of high $[Ca^{2+}]_o$, the ability of the calcimimetic, R-568, to modulate terminal lung branching was tested. Figure 2*C* shows that 10 nM R-568, administered in the presence of maximally permissive $[Ca^{2+}]_o$ (i.e. 1.2 mM), reduced branching morphogenesis at 48 h to levels not significantly different ($P > 0.2$) from those observed in the presence of 1.7 mM $[Ca^{2+}]_o$ (i.e. 75.0% ± 10.2, $n = 9$ *versus* 62.2 ± 4.4%, $n = 45$, respectively); see Fig. 4*A* for representative images of the effects of R-568.

Inhibition of phospholipase C (PLC) abrogates the effects of high $[Ca^{2+}]_o$ on lung branching morphogenesis

To provide further evidence that the observed effects of $[Ca^{2+}]_o$ on lung branching were downstream of an activation of a GPCR, namely the CaR, explants were cultured in the presence of 5 μM of the PLC inhibitor, U73122, and branching was assessed at 24 and 48 h. Since U73122 was dissolved in DMSO (final concentration 0.1%, v/v), paired vehicle-control experiments were performed. In the presence of 0.1% DMSO, the increase in branching in 1.05 mM $[Ca^{2+}]_o$ was 108.0 ± 8.3% while in 1.7 mM $[Ca^{2+}]_o$ it was 54.0 ± 11.6% (Fig. 3*A* and *B*, left panels). These data are not different from those obtained in the absence of DMSO (see Fig. 2 for comparison). Therefore, independently of DMSO, branching in the presence of 1.05 mM Ca_o^{2+} was always between ∼2 and 2.5-fold higher than that observed in the presence of 1.7 mM Ca_o^{2+}.

At 24 h, branching in the presence of 1.05 mM Ca_o^{2+} was significantly increased by 5 μM U73122 (from 20.5 ± 4.6% in its absence to 54 ± 8.1% in its presence – Fig. 3*A* and *B*), suggesting that CaR, via PLC, tonically suppressed branching at 1.05 mM Ca_o^{2+}. This is not surprising since the EC_{50} of the CaR is above 1 mM in all systems thus far studied (Brown & Macleod, 2001). At 48 h, in the presence of 1.05 mM Ca_o^{2+} this de-repressive effect of

Figure 1. CaR ontogeny in the mouse lung
CaR protein expression was detected using an affinity-purified, rabbit polyclonal antiserum (733) directed against a peptide in the N-terminal region of the receptor and shows that the CaR is expressed within a narrow developmental window. CaR immunoreactivity was detected mostly in the lung epithelium at E10.5 (*A*), E11.5 (*B*), E12.5 (*C*) and E13.5 (*D*) and then subsequently also in the mesenchyme from E14.5 (*E*), E16.5 (*F*) and E18.5 (*G*), but with progressively decreasing intensity. At P0 (*H*) and in the adult (*I*), CaR expression was no longer detectable. Arrows: epithelium. Arrowheads: mesenchyme. Bars = 50 μm. Using antiserum IMG-71169, CaR protein was also detected in the epithelium of E12.5 lungs cultured for 48 h (*J*). *K* shows a serial section from the same lung as that depicted in *J*, where the preimmune serum was used (negative control). Exemplar quantitative PCRs from 2 separate experiments ($n = 3$–5 lungs per developmental time point) are in agreement with the immunohistochemistry data and confirm a peak of CaR mRNA expression at E12.5 and the absence of CaR mRNA in postnatal mice (*L*). Bars = 100 μm (*J* and *K*).

U73122 persisted (Fig. 3*A* and *B*). A more dramatic effect of PLC inhibition was apparent with 5 μM U73122 in the presence of 1.7 mM Ca_o^{2+}, a concentration which activates maximally the CaR. Thus, in the absence of PLC inhibition, 1.7 mM Ca_o^{2+} evoked the expected repression of branching (Fig. 3*A* and *B*) but, most importantly, in the presence of the PLC inhibitor, branching at both 24 and 48 h was fully restored to levels normally associated with lower $[Ca^{2+}]_o$ (Fig. 3*A* and *B*). For example, at 48 h, the expected decrease in branching evoked by high $[Ca^{2+}]_o$ (from 108 ± 8.3% to 54.0 ± 11.6%) was completely reversed by U73122 so that the increase in branching was restored to 150.2 ± 22.9%, a value which was not significantly different from that seen in low $[Ca^{2+}]_o$ in the presence of U73122 (156.3 ± 23.1%). Thus, experimental inhibition of PLC resulted in the lung branching programme becoming completely insensitive to $[Ca^{2+}]_o$.

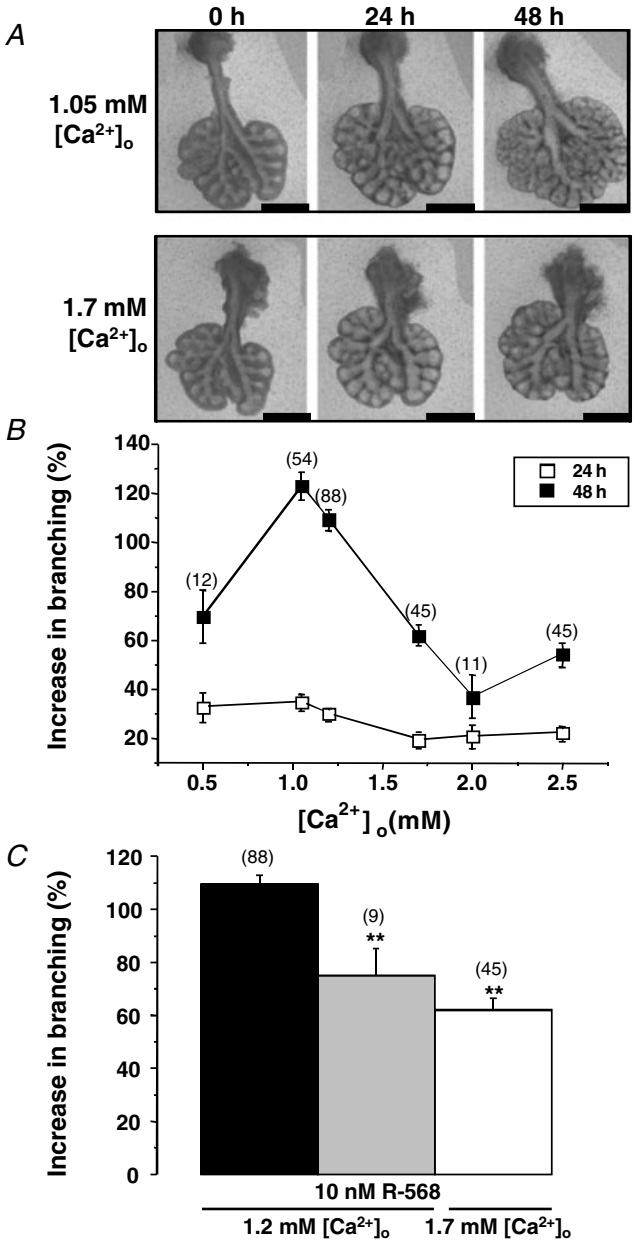

Figure 2. $[Ca^{2+}]_o$ and CaR dependence of lung branching morphogenesis
A, effect of either 1.05 mM (upper panel) or 1.7 mM (lower panel) Ca_o^{2+} on branching by E12.5 lungs at $t = 0$ h (left), $t = 24$ h (middle) and $t = 48$ h (right) in culture. Quantification of branching at 24 (□) and 48 h (■) of E12.5 lungs in the $[Ca^{2+}]_o$ indicated on the abscissa. Bar = 700 μm. *B*, effect of 1.7 mM $[Ca^{2+}]_o$ and 10 nM of the calcimimetic R-568 on branching. *C*, high $[Ca^{2+}]_o$ suppresses branching and this inhibitory effect was mimicked by R-568. Data pooled from ≥ 25 independent isolations. Asterisks indicate significantly different ($P < 0.01$) from 1.2 mM $[Ca^{2+}]_o$.

CaR agonists evoke an increase in $[Ca^{2+}]_i$ signalling in the epithelium of E12.5 lungs

In most cell types studied to date, activation of the G protein-coupled CaR by its agonists causes PLC-evoked Ca_i^{2+} release from internal stores (see, for example Brown *et al.* 1993). To test the hypothesis that the CaR in the developing lung epithelium is functional, Ca_i^{2+} homeostasis was studied in isolated epithelial buds of E12.5 lung explants. CaR is exclusively expressed in the epithelium at this time-point (see Fig. 1). When $[Ca^{2+}]_o$ was increased from 0.8 to 2 mM, the mean increase in Fura-2 340/380 ratio increased transiently by 0.18 ± 0.04 (Fig. 3*C*). The figure also shows that, in the presence of 0.8 mM Ca_o^{2+}, 100 nM R-568 evoked a mean increase of 0.090 ± 0.02. At the end of each experiment, and as a control for viability of the preparation, isolated epithelial buds were treated with 10 μM carbachol, an activator of muscarinic acetylcholine receptors, which we here show to be expressed in developing mouse lungs (mean increase in Fura-2 340/380 ratio of 0.16 ± 0.02 – Fig. 3*C*). Taken together, the data in Fig. 3 show that both Ca_o^{2+} and the membrane-impermeant R-568 evoke Ca_i^{2+} release and that Ca_o^{2+} depresses lung branching via PLC activation. These characteristics suggest strongly that the mouse lung CaR is functionally active and coupled to PLC–IP_3–Ca_i^{2+} signalling.

PI3 kinase inhibition also rescues the effects of high $[Ca^{2+}]_o$ on lung branching morphogenesis

In many cellular systems the CaR is linked to its biological effectors via mitogen-activated protein kinase (MAPK) and PI3K signalling. The role of each of these signalling pathways was tested by studying the effects of well-characterized MAPK and PI3K blockers on both Ca_o^{2+}- and calcimimetic-evoked suppression of branching. None of the MAPK signalling inhibitors – 1 μM BIRB796 to inhibit p38 MAPK ($n = 7$), 25 and 50 μM PD98059 to inhibit MEK ($n = 17$), 20 and 30 μM U0126 to inhibit

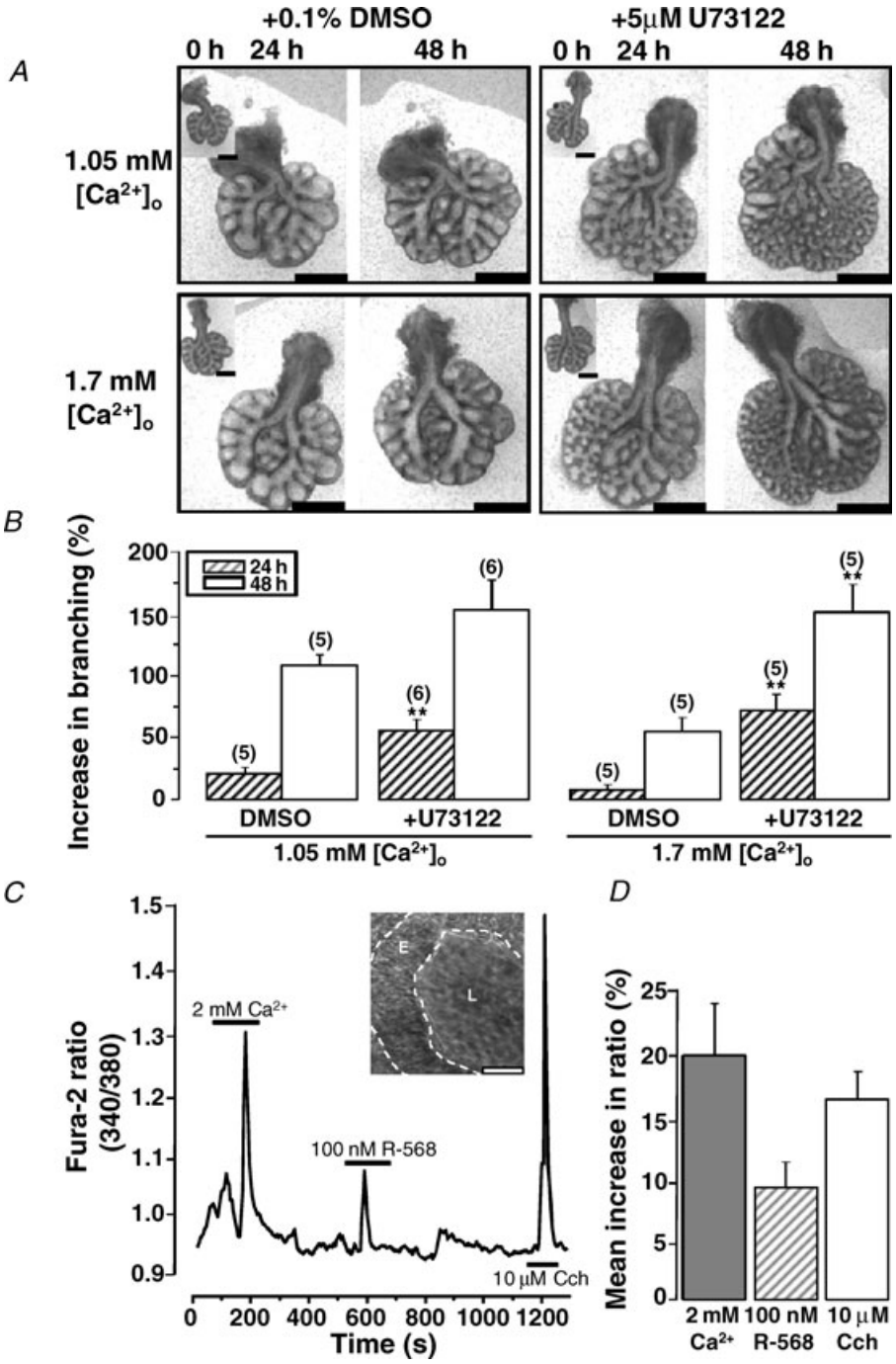

Figure 3. Evidence for CaR-evoked, PLC-dependent branching and $[Ca^{2+}]_i$ signalling
A and *B*, effect of either 1.05 mM (*A*, upper panels) or 1.7 mM (*A*, lower panels) Ca_o^{2+} in the absence (0.1% DMSO vehicle control; *A* left panels and *B*) or presence (*A* right panels and *B*) of 5 μM of the PLC inhibitor, U73122, on branching. The quantification of branching in the 4 conditions ($n = 5$ lungs per condition from ≥ 2 isolations) at 24 and 48 h is shown in *B*. Inhibition of PLC completely rescued the suppression of branching which was evoked by 1.7 mM Ca_o^{2+}. Asterisks indicate that values are significantly different ($P < 0.01$) from their time-matched DMSO controls. *C*, exemplar time course showing that that CaR-expressing epithelial cells exhibited rapid and transient increases in $[Ca^{2+}]_i$ (340 : 380 fura-2 fluorescence ratio) in response to acute (1–3 min) stimulation with Ca_o^{2+} (2 mM), and with the calcimimetic compound R-568 (100 nM). Carbachol treatment (Cch, 10 μM) confirmed cell viability at the end of the experiment. Inset shows the epithelial layer from which the recordings were made; E epithelium; L = lumen. Bar = 200 μm. *D*, mean increases in fura-2 fluorescence ratio (6 epithelial buds from three separate isolations performed on three different days of experimentation). Bars = 700 μm (*A*) or 50 μm (*C*).

ERK1/2 ($n = 12$) – were able to rescue the inhibitory effects of high Ca_o^{2+} on branching morphogenesis (not shown). In contrast, the PI3K inhibitor LY294002 was able to rescue completely the inhibitory effects of both high Ca_o^{2+} and the calcimimetic on branching morphogenesis (Fig. 4*A* and *B*). Thus, at 48 h, the increase in branching in the presence of 1.05 mM Ca_o^{2+} was 135.2 ± 19.9% and this was reduced to 76.2 ± 12.7% by 30 nM R-586; this inhibition was completely reversed by the co-addition of 12.5 μM LY294002 so that branching was restored

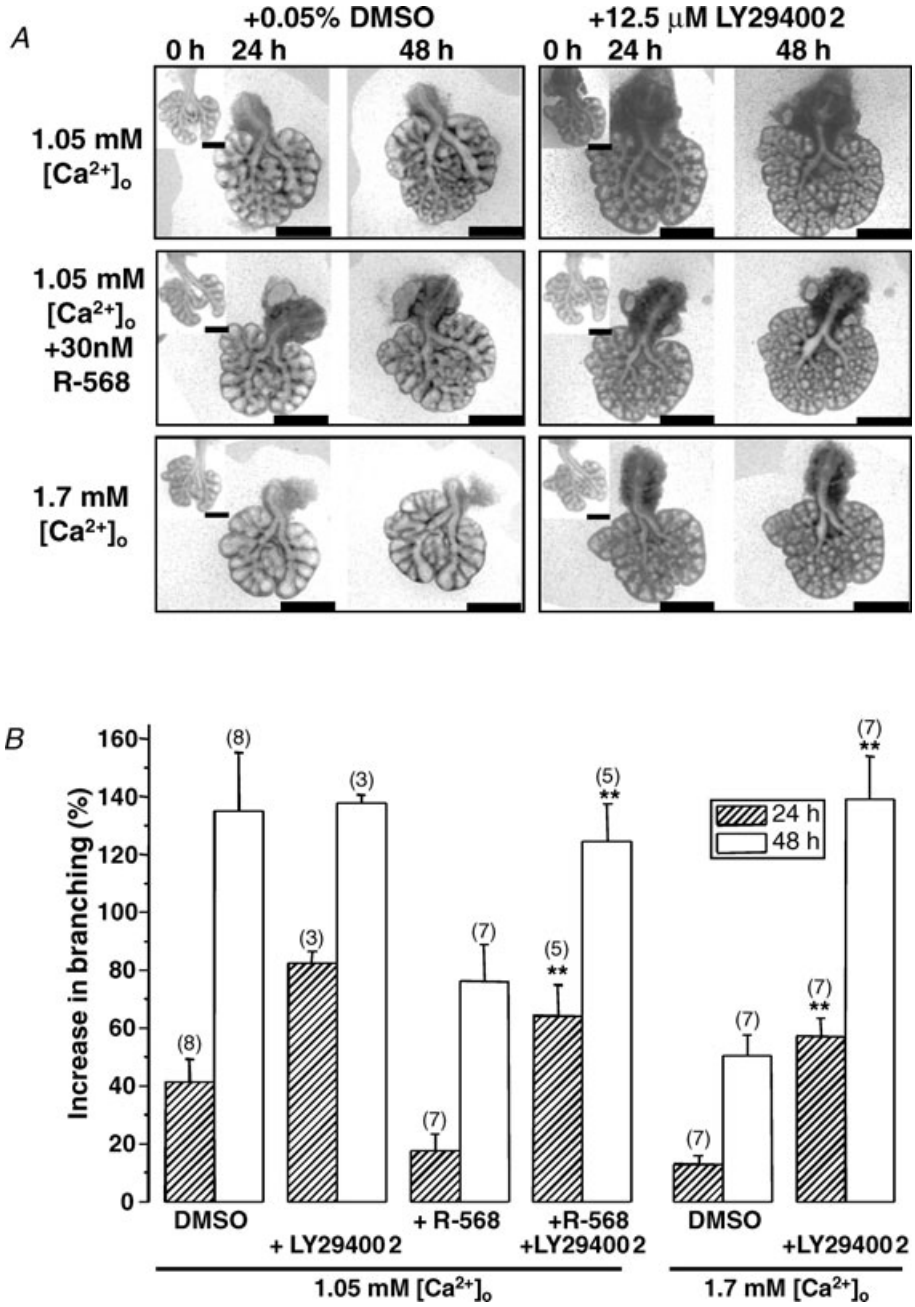

Figure 4. Effect of inhibition of PI3 kinase on $[Ca^{2+}]_o$- and calcimimetic-regulated branching morphogenesis
A, effect of 1.05 mM Ca_o^{2+} (upper panels), 1.05 mM Ca_o^{2+} plus 30 nM R-568 (middle panels) and 1.7 mM Ca_o^{2+} (lower panels) in the absence (0.05% DMSO vehicle control – 1st and 2nd panels) or presence (3rd and 4th panels) of 12.5 μM of the PI3K inhibitor LY294002 on branching. Bar = 750 μm. *B*, mean percentage change in branching at 24 and 48 h. Rescue by LY294002 of the inhibition of branching which was evoked by either R-568 or 1.7 mM Ca_o^{2+} is indicated in time-matched samples by the asterisks (**$P < 0.01$).

to 124.5 ± 13.7%. Furthermore, this PI3K inhibitor also rescued the suppression of branching, which was evoked by 1.7 mM Ca_o^{2+} (from 50.5 ± 7.0 to 139.2 ± 14.7). As expected from the data shown in Fig. 3, 0.05% DMSO did not effect the ability of high Ca_o^{2+} to suppress branching (Fig. 4*A*, left panels and *B*). These results suggest that PI3K inhibition renders the embryonic lung branching developmental programme insensitive to Ca_o^{2+}.

CaR activation stimulates lung distension

Fluid-dependent embryonic lung distension is necessary for adequate lung growth (Moessinger *et al.* 1990). To investigate how $[Ca^{2+}]_o$ affects lung growth, time-lapse images of cultured lung explants were recorded for 48 h. Figure 5*A* illustrates that both the rate and extent of branching were dramatically reduced in the presence of the high $[Ca^{2+}]_o$. The figure also shows that in addition to a reduction in the number of terminal branches, lung explants incubated in a high $[Ca^{2+}]_o$ were more distended and exhibited a higher luminal volume, indicative of an increased lung fluid secretion.

Embryonic lung fluid secretion is driven by secondary active Cl^- transport (Olver & Strang, 1974). This results in a negative transepithelial potential difference (PD). Therefore, the magnitude of the transepithelial PD reflects the rate of Cl^--driven fluid secretion. Measurement of transepithelial PD has not been previously reported in a mouse culture model of lung branching. The mean transepithelial PD of terminal branches from lungs cultured for 48 h in 1.05 mM Ca_o^{2+} was −1.2 ± 0.1 mV. The mean PD in 1.7 mM Ca_o^{2+} was significantly more negative at −1.7 ± 0.2 mV (Figs 5*B*, $n \geq 17$, $P < 0.05$). Furthermore, specific activation of CaR with 30 nM R-568 in the presence of 1.05 mM Ca_o^{2+} also promoted the generation of a significantly more negative PD (−2.2 ± 0.1 mV, $n = 4$, $P = 0.007$ – Fig. 5*B*), showing that CaR activation stimulates transepithelial electrogenic transport. The increased fluid secretion, which would be expected to accompany such increased lumen negativity, may go some way to explaining how CaR activation leads to increased lung distension even in the presence of decreased branching (see Fig. 5*A* and Fig. 6*B*).

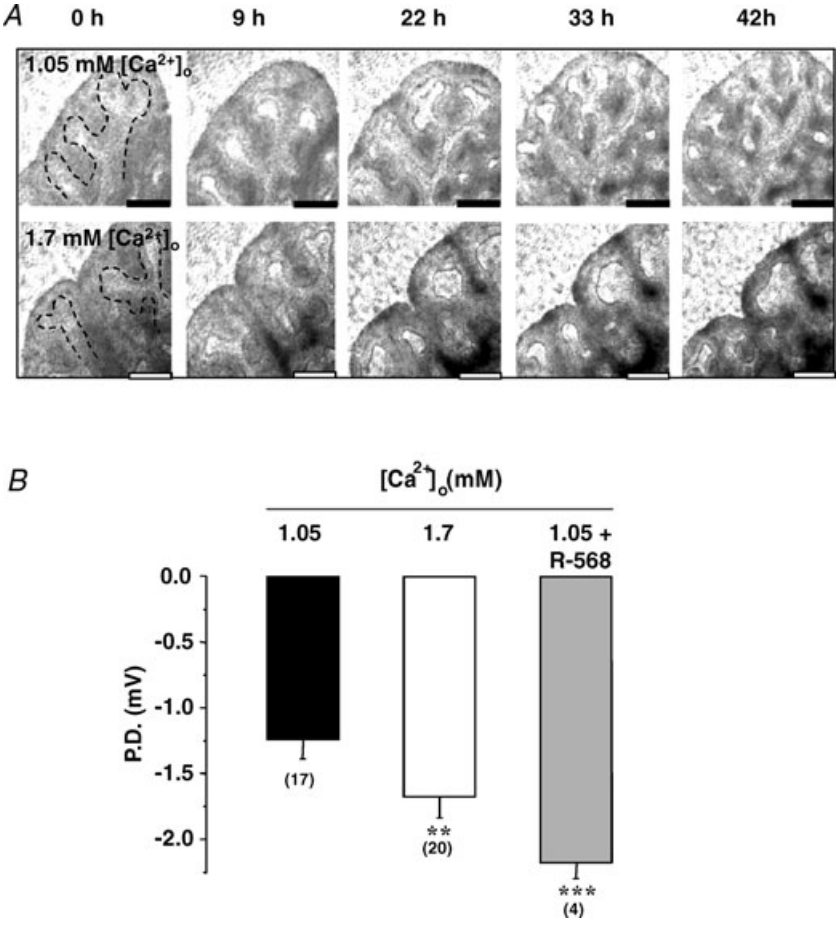

Figure 5. Effects of CaR activation on lung distension and transepithelial potential difference
A, images were taken from time-lapse sequences of E12.5 lung explants grown for up to 48 h on transwell supports and exposed to either 1.05 mM (upper panels) or 1.7 mM (lower panels) Ca_o^{2+} at the times in culture indicated below each pair of images. The dashed lines delineate the lumen. Bar = 100 μm. *B*, mean transepithelial potential differences (PD) of terminal branches of E12.5 lungs cultured for 48 h in the presence of 1.05 mM (± 30 nM R-568) or 1.7 mM Ca_o^{2+}, as indicated below the bars. CaR activation promotes both distension and fluid secretion whilst suppressing branching. $^{**}P < 0.01$. $^{***}P < 0.001$.

High $[Ca^{2+}]_o$ inhibits lung cell proliferation but does not affect apoptosis

A reduction in lung branching morphogenesis could be the consequence of (a) decreased proliferation, (b) increased apoptosis, or (c) a combination of both. Figure 6 confirmed that 1.7 mM Ca_o^{2+} decreased branching compared to 1.05 mM Ca_o^{2+} (Fig. 6*A*) and that this effect was accompanied by a high level of expansion and an increase in the lumenal volume (Fig. 6*B*), as predicted from the increased transepithelial PD (see Fig. 5*B*). In lungs incubated for 48 h in the presence of 1.05 mM Ca_o^{2+}, the percentage of phospho-histone H3-positive cells was $11.5 \pm 0.4\%$ whilst in 1.7 mM Ca_o^{2+} this was significantly ($n = 3$, $P < 0.001$) reduced to $5.4 \pm 0.9\%$ (Fig. 6*B* and *D*). In contrast, there was no significant difference between the number of apoptotic cells in sections from lung explants kept in low *versus* high Ca_o^{2+} (Fig. 6*C* and *D*).

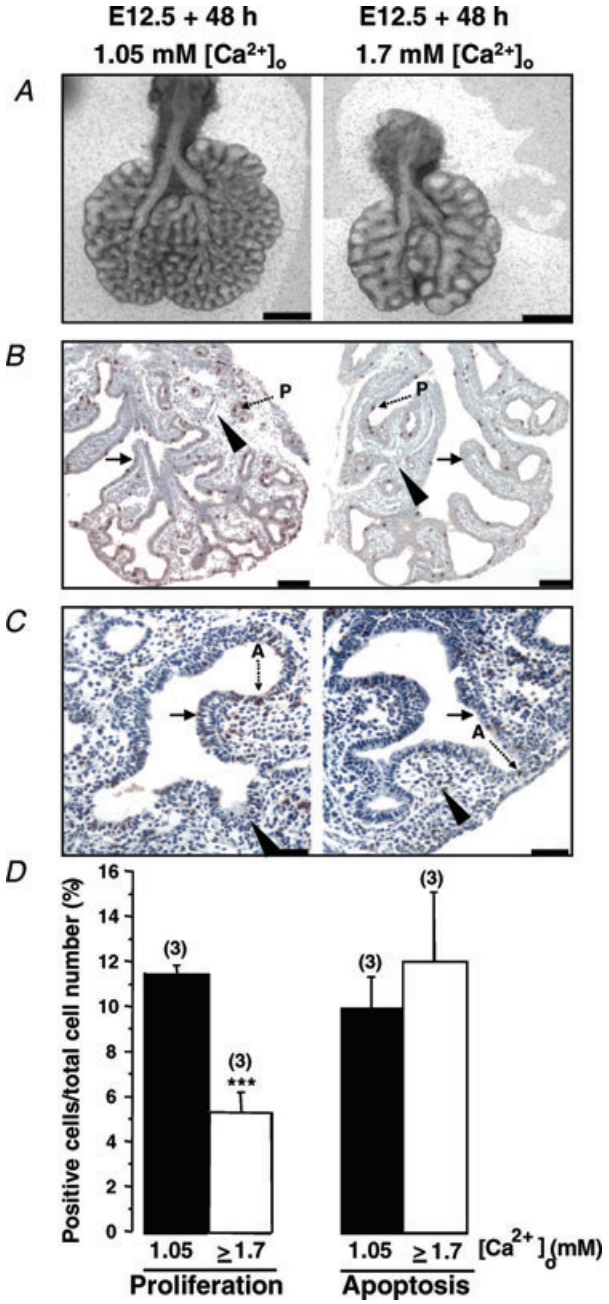

Figure 6. $[Ca^{2+}]_o$-dependent effects on proliferation and apoptosis
A–C, effect of 1.05 mM Ca_o^{2+} (left panels) and $\geq$ 1.7 mM Ca_o^{2+} (right panels) on branching (*A*), proliferation (phospho-histone H3 antibody – *B*) and apoptosis (TUNEL staining – *C*) on E12.5 lungs cultured for 48 h. Bars are 500 μm (*A*) and 100 μm (*B* and *C*). P indicates exemplar proliferating cell, A indicates exemplar apoptotic cell, arrow is epithelium and arrowhead is mesenchyme. *D*, mean percentage of positive cells under each experimental condition, as indicated below the bars.

Manipulation of $[Ca^{2+}]_o$ rescues inhibitory branching and secretion signals

Finally, the ability of $[Ca^{2+}]_o$ to affect permanently the intrinsic lung developmental programme(s) which control branching morphogenesis and secretion was investigated. After 24 h in culture, lung explants were switched from 1.05 mM $[Ca^{2+}]_o$ to 1.7 mM $[Ca^{2+}]_o$, or *vice versa*. The consequences of these switching protocols on lung branching morphogenesis and transepithelial PD were assayed after a further 24 h. Figure 7 shows that when lungs were switched from 1.05 mM to 1.7 mM Ca_o^{2+}, branching was not affected ($172.6 \pm 30.7\%$ increase in branching in lungs kept in 1.05 mM Ca_o^{2+}, *versus* $171.8 \pm 22.4\%$ in lungs switched from 1.05 to 1.7 mM – Fig. 7*A* 2nd panel and *B*, $n = 5$). In contrast, transepithelial PD was increased from -1.1 ± 0.1 to -1.5 ± 0.2 mV by switching from low to high $[Ca^{2+}]_o$, a value not different from that recorded in lungs cultured constantly in 1.7 mM Ca_o^{2+} (Fig. 7*C*). Importantly, the expected suppressive effects of high $[Ca^{2+}]_o$ on branching could be completely rescued by switching the lung from 1.7 mM into 1.05 mM Ca_o^{2+} (Fig. 7*A*, 4th panel and *B*). When lungs were cultured in 1.7 mM Ca_o^{2+} for 48 h, the increase in branching was only $80.8 \pm 20.7\%$ (Fig. 7*A*, 3rd panel and *B*), but switching at 24 h from 1.7 mM to 1.05 mM Ca_o^{2+} supported a full restoration to $154.6 \pm 19.6\%$ (Fig. 7, 4th panel and *B*, $n = 5$), a value not statistically different from those obtained in either low Ca_o^{2+} or low Ca_o^{2+} switched to high Ca_o^{2+}. Interestingly, transepithelial PD was not affected by the switch from 1.7 mM to 1.05 mM, with values of -1.4 ± 0.2 mV in 1.7 mM Ca_o^{2+} *versus* -1.4 ± 0.2 mV following the switch from 1.7 mM to 1.05 mM Ca_o^{2+}; $n = 5$ lungs per condition – Fig. 7*C*. These data show that suppression of branching can be rescued by manipulating Ca_o^{2+}. They also show that that secretion does not drive lung branching even though is does stimulate lung growth.

Discussion

Many adult respiratory pathologies are associated with an impaired growth and maturation of the lung *in utero*

(Shi *et al.* 2007). The present study has demonstrated that serum Ca^{2+} is a key physiological determinant of embryonic lung morphogenesis, and that these effects are mediated through a developmentally regulated CaR. The narrow window of expression of the receptor is coincident with the time during which lung branching morphogenesis takes place, suggesting that the CaR is involved in the regulation of both peripheral tubule formation and airway expansion. Interestingly, Ca_o^{2+} regulates these two events in an opposite manner. Indeed, Ca_o^{2+} has a dramatic effect on branching morphogenesis, with the physiological adult $[Ca^{2+}]_o$ being the most permissive and the physiological fetal $[Ca^{2+}]_o$ having a repressive effect. In contrast, fetal $[Ca^{2+}]_o$ enhances fluid secretion and evokes lung distension to a greater extent than adult $[Ca^{2+}]_o$. That the CaR is involved in mediating the effects of high $[Ca^{2+}]_o$ has been demonstrated in three ways. Firstly, at the concentrations used by us (i.e. 10–100 nM), the calcimimetic R-568 mimics the effect of high $[Ca^{2+}]_o$ on both branching morphogenesis and fluid secretion, directly implicating CaR activation in both processes. Secondly, both $[Ca^{2+}]_o$ and the membrane-impermeant R-568 trigger an increase in $[Ca^{2+}]_i$, a response which is typical of CaR activation (Brown & Macleod, 2001). Thirdly, inhibition of two known downstream effectors of the CaR, PLC (Brown *et al.* 1993) and PI3K (Tu *et al.* 2008), rescue the suppression of lung branching morphogenesis which is induced both by high $[Ca^{2+}]_o$ and by the calcimimetics. This strongly suggests that the inhibitory effects of high $[Ca^{2+}]_o$ on branching are primarily due to activation of this G protein-coupled receptor, rather than to Ca^{2+} ions crossing the plasma membrane through Ca^{2+} channels. Taken together, our results lend further credibility to the hypothesis that the developing mouse lung expresses a functional CaR, which mediates the effects of both Ca^{2+} and calcimimetics on lung branching morphogenesis.

Previous studies have demonstrated that Ca_o^{2+}-induced differentiation of epidermal keratinocytes is mediated by the CaR through activation of the E cadherin–PI3K pathway (Tu *et al.* 2008). In that study the authors showed that CaR activation led to formation of an

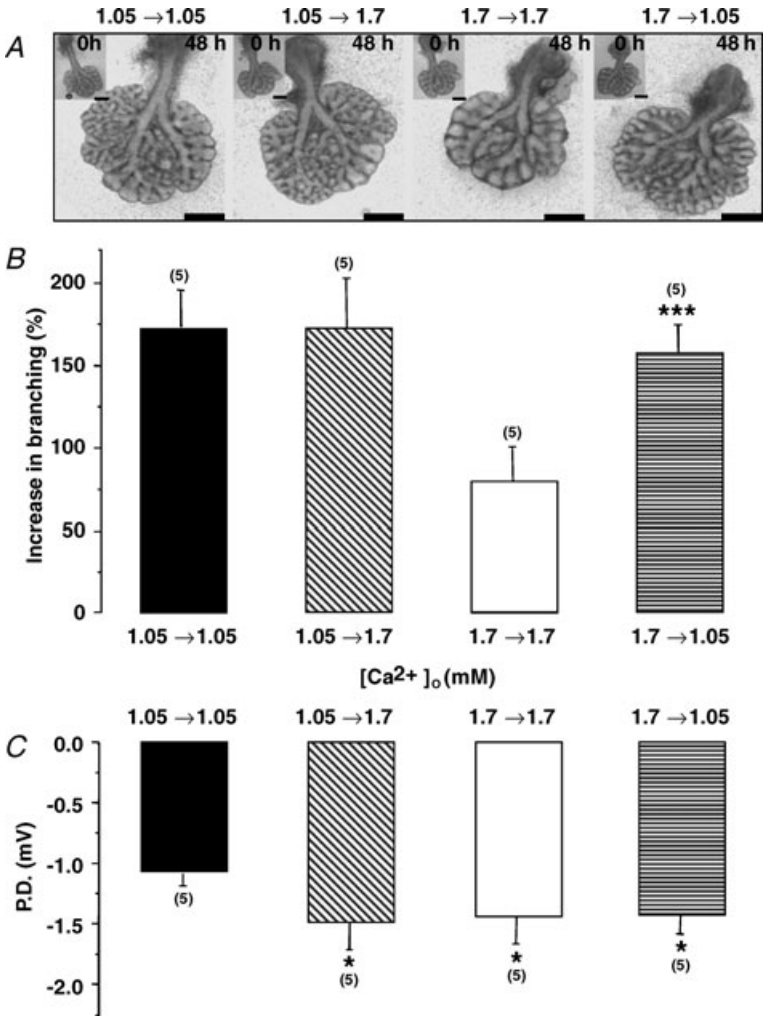

Figure 7. Effect of switching Ca_o^{2+} on branching and transepithelial PD
A, E12.5 lung explants were cultured for 24 h in 1.05 mM (1st and 2nd panels) or 1.7 mM (3rd and 4th panels) and then transferred to wells containing either the same $[Ca^{2+}]_o$ (1st and 3rd panels) or a different $[Ca^{2+}]_o$ (2nd and 4th panels), as indicated. *B* and *C*, mean branching at 48 h under each condition are shown in *B* ($n \geq 10$ per condition) whilst mean transepthelial PD under each condition are shown in *C* ($n = 5$ lungs per condition). Switching from 1.7 mM to 1.05 mM Ca_o^{2+} rescued the normal suppression of branching but left PD unaffected. In contrast, switching from 1.05 to 1.7 mM Ca_o^{2+} was unable to inhibit branching but augmented PD. Bar = 600 μm.

E-cadherin–catenin complex, PI3K activation, activation of PLC and a subsequent increase in $[Ca^{2+}]_i$, which is ultimately necessary for Ca_o^{2+}-induced keratinocyte differentiation. In the developing mouse lung, we propose that CaR activation is coupled to recruitment of PI3K to the plasma membrane and/or attendant PLC activation, with an increase in Ca_i^{2+}. Alone or in combination, these two events suppress branching while stimulating distension. The integration of both inhibitory and stimulatory signals ultimately results in an optimal number of distended branches when $[Ca^{2+}]_o$ is close to that measured in the fetus. Failure to achieve this equilibrium yields pathological manifestations, as evidenced by the fact that both hypoplastic and hyperplastic lungs impair pulmonary function (Nakamura *et al.* 1992; Mori *et al.* 2001).

This study shows that suppression of lung branching morphogenesis by high $[Ca^{2+}]_o$ is achieved principally by a decrease in cell proliferation, rather than an increase in apoptosis. We have recently shown that activation of the CaR using calcimimetics reduces parathyroid cell proliferation by altering the expression of the cell cycle inhibitor p21 (Riccardi & Martin, 2008). Thus, we speculate that CaR stimulation in the developing lung could inhibit the activity of cyclin-dependent kinase(s), thereby controlling cell cycle entry. Indeed, failure to control excessive proliferation could result in hyperplastic lungs and could account for the respiratory problems encountered by some familial hypocalciuric hyperpercalcaemia patients (Fox *et al.* 2007). On the other hand, autosomal dominant hypocalcaemia due to activating mutations in the CaR is linked with ectopic calcification in the mouse lung (Hough *et al.* 2004) with evidence of recurrent upper respiratory infections in humans (Hu *et al.* 2004). These observations suggest that both hypocalcaemia and hypercalcaemia are associated with an impaired lung function. Further longitudinal studies are necessary to test the incidence of respiratory pathologies in the infant and adult population in familial hypocalciuric hyperpercalcaemia and/or autosomal dominant hypocalcaemia patients.

Overall, our study shows that fetal $[Ca^{2+}]_o$ may exert a physiological brake on branching morphogenesis while stimulating lung fluid secretion, potentially to allow for lung development to proceed in parallel with optimal lumen distension and/or adequate fluid secretion. Interestingly, it has been suggested that lumen distension caused by the accumulation of fluid disrupts lung branching morphogenesis (Nogawa & Hasegawa, 2002). However, our experiments where $[Ca^{2+}]_o$ was switched after the initial 24 h culture period would argue against this being the primary mechanism for inhibition of branching by CaR activation.

In conclusion, lung branching morphogenesis and secretory driving force are exquisitely sensitive to $[Ca^{2+}]_o$. At fetal $[Ca^{2+}]_o$, branching is tonically suppressed whilst secretion is activated. This results in optimal matching of branching and distension. PI3K signalling, possibly via $[Ca^{2+}]_i$ mobilization, regulates embryonic lung development, suggesting that both extracellular and intracellular Ca^{2+} signals must be coupled and tightly controlled in order for fetal lung development to progress optimally. These processes are entirely dependent on developmentally regulated expression of CaR in the epithelium. If these findings hold true for humans, they present the intriguing possibility of using pharmacological manipulators of the CaR to rescue hypoplastic/hyperplastic lung disease in premature babies.

References

Auwerx J, Brunzell J, Bouillon R & Demedts M (1987). Familial hypocalciuric hypercalcaemia – familial benign hypercalcaemia: a review. *Postgrad Med J* **63**, 835–840.

Auwerx J, Demedts M, Bouillon R & Desmet J (1985). Coexistence of hypocalciuric hypercalcaemia and interstitial lung disease in a family: a cross-sectional study. *Eur J Clin Invest* **15**, 6–14.

Brown EM (1991). Extracellular Ca^{2+} sensing, regulation of parathyroid cell function, and role of Ca^{2+} and other ions as extracellular (first) messengers. *Physiol Rev* **71**, 371–411.

Brown EM, Gamba G, Riccardi D, Lombardi M, Butters R, Kifor O, Sun A, Hediger MA, Lytton J & Hebert SC (1993). Cloning and characterization of an extracellular Ca^{2+}-sensing receptor from bovine parathyroid. *Nature* **366**, 575–580.

Brown EM & Macleod RJ (2001). Extracellular calcium sensing and extracellular calcium signaling. *Physiol Rev* **81**, 239–297.

Bruce JI, Yang X, Ferguson CJ, Elliott AC, Steward MC, Case RM & Riccardi D (1999). Molecular and functional identification of a Ca^{2+} (polyvalent cation)-sensing receptor in rat pancreas. *J Biol Chem* **274**, 20561–20568.

De Langhe SP, Sala FG, Del Moral PM, Fairbanks TJ, Yamada KM, Warburton D, Burns RC & Bellusci S (2005). Dickkopf-1 (DKK1) reveals that fibronectin is a major target of Wnt signaling in branching morphogenesis of the mouse embryonic lung. *Dev Biol* **277**, 316–331.

Del Moral PM, Sala FG, Tefft D, Shi W, Keshet E, Bellusci S & Warburton D (2006). VEGF-A signaling through Flk-1 is a critical facilitator of early embryonic lung epithelial to endothelial crosstalk and branching morphogenesis. *Dev Biol* **290**, 177–188.

Dvorak MM, Siddiqua A, Ward DT, Carter DH, Dallas SL, Nemeth EF & Riccardi D (2004). Physiological changes in extracellular calcium concentration directly control osteoblast function in the absence of calciotropic hormones. *Proc Natl Acad Sci U S A* **101**, 5140–5145.

Fox L, Sadowsky J, Pringle KP, Kidd A, Murdoch J, Cole DE & Wiltshire E (2007). Neonatal hyperparathyroidism and pamidronate therapy in an extremely premature infant. *Pediatrics* **120**, e1350–e1354.

Hough TA, Bogani D, Cheeseman MT, Favor J, Nesbit MA, Thakker RV & Lyon MF (2004). Activating calcium-sensing receptor mutation in the mouse is associated with cataracts and ectopic calcification. *Proc Natl Acad Sci U S A* **101**, 13566–13571.

Hu J, Mora S, Weber G, Zamproni I, Proverbio MC & Spiegel AM (2004). Autosomal dominant hypocalcemia in monozygotic twins caused by a de novo germline mutation near the amino-terminus of the human calcium receptor. *J Bone Miner Res* **19**, 578–586.

Kovacs CS, Ho-Pao CL, Hunzelman JL, Lanske B, Fox J, Seidman JG, Seidman CE & Kronenberg HM (1998). Regulation of murine fetal-placental calcium metabolism by the calcium-sensing receptor. *J Clin Invest* **101**, 2812–2820.

Kovacs CS & Kronenberg HM (1997). Maternal-fetal calcium and bone metabolism during pregnancy, puerperium, and lactation. *Endocr Rev* **18**, 832–872.

Moessinger AC, Harding R, Adamson TM, Singh M & Kiu GT (1990). Role of lung fluid volume in growth and maturation of the fetal sheep lung. *J Clin Invest* **86**, 1270–1277.

Mori K, Ikeda K, Hayashida S, Tokieda K, Ishimoto H, Fujii Y, Fukuzawa R & Kitano Y (2001). Pulmonary epithelial cell maturation in hyperplastic lungs associated with fetal tracheal agenesis. *J Pediatr Surg* **36**, 1845–1848.

Nakamura Y, Harada K, Yamamoto I, Uemura Y, Okamoto K, Fukuda S & Hashimoto T (1992). Human pulmonary hypoplasia. Statistical, morphological, morphometric, and biochemical study. *Arch Pathol Laboratory Med* **116**, 635–642.

Nogawa H & Hasegawa Y (2002). Sucrose stimulates branching morphogenesis of embryonic mouse lung in vitro: a problem of osmotic balance between lumen fluid and culture medium. *Dev Growth Differ* **44**, 383–390.

Olver RE & Strang LB (1974). Ion fluxes across the pulmonary epithelium and the secretion of lung liquid in the foetal lamb. *J Physiol* **241**, 327–357.

Riccardi D, Hall AE, Chattopadhyay N, Xu JZ, Brown EM & Hebert SC (1998). Localization of the extracellular Ca^{2+}/polyvalent cation-sensing protein in rat kidney. *Am J Physiol Renal Physiol* **274**, F611–F622.

Riccardi D & Martin D (2008). The role of the calcium-sensing receptor in the pathophysiology of secondary hyperparathyroidism. *Nephron Dial Transplant Plus* **1**, 7–11.

Riccardi D, Park J, Lee WS, Gamba G, Brown EM & Hebert SC (1995). Cloning and functional expression of a rat kidney extracellular calcium/polyvalent cation-sensing receptor. *Proc Natl Acad Sci U S A* **92**, 131–135.

Shi W, Bellusci S & Warburton D (2007). Lung development and adult lung diseases. *Chest* **132**, 651–656.

Tu CL, Chang W, Xie Z & Bikle DD (2008). Inactivation of the calcium sensing receptor inhibits E-cadherin-mediated cell-cell adhesion and calcium-induced differentiation in human epidermal keratinocytes. *J Biol Chem* **283**, 3519–3528.

Vizard TN, O'Keeffe GW, Gutierrez H, Kos CH, Riccardi D & Davies AM (2008). Regulation of axonal and dendritic growth by the extracellular calcium-sensing receptor. *Nat Neurosci* **11**, 285–291.

Warburton D (2008). Developmental biology: order in the lung. *Nature* **453**, 733–735.

Warburton D & Olver RE (1997). Coordination of genetic, epigenetic, and environmental factors in lung development, injury, and repair. *Chest* **111**, S119–S122.

Ward DT, McLarnon SJ & Riccardi D (2002). Aminoglycosides increase intracellular calcium levels and ERK activity in proximal tubular OK cells expressing the extracellular calcium-sensing receptor. *J Am Soc Nephrol* **13**, 1481–1489.

Whitsett JA, Wert SE & Trapnell BC (2004). Genetic disorders influencing lung formation and function at birth. *Hum Mol Genet* **13** Spec No 2, R207–R215.

Acknowledgements

This work was funded by the Biotechnology and Biological Sciences Research Council (grant BB/D01591X, to D.R. and P.J.K.), and also by NIH grants PO1HL60231, HL44060, HL75773 and HL44977 to D.W. and an AHA Postdoctoral Fellowship to P.M.dM. as well as the Pasadena Guild Developmental Biology Endowment and funds from the Saban Research Institute. We thank Dr J. Ralphs for help with microscopy and Dr M. Bagley for the kind gift of BIRB796, both of Cardiff University.